J. A. Joyce and E. M. Hackett†*

Development of an Engineering Definition of the Extent of *J*-Controlled Crack Growth

REFERENCE Joyce, J. A. and Hackett, E. M., **Development of an engineering definition of the extent of *J*-controlled crack growth**, *Defect Assessment of Components – Fundamentals and Applications*, ESIS/EGF9 (Edited by J. G. Blauel and K.-H. Schwalbe) 1991, Mechanical Engineering Publications, London, pp. 233–249.

ABSTRACT An experimental definition is proposed for the extent of *J*-integral controlled behaviour in a *J*-resistance fracture test. The *J*-control zone is defined in terms of a constant ratio of plastic crack opening displacement and normalised crack extension. Justification for this definition is given in terms of experimental results on compact specimens of three steel alloys of varying material toughnesses.

The experimental limit can be evaluated from the data normally obtained during an unloading compliance single specimen *J*-integral resistance curve experiment. Generally the experimental singularity limit extends the region of test validity well beyond that which is presently allowed by the ASTM *J–R* test standard, E1152.

Notation

a	Crack length
a_i	Crack length at loading step i
a_0	Initial crack length
A_{pl}	Plastic component of the area
b	Uncracked ligament $(W-a)$
b_i	Uncracked ligament at loading step i
B	Specimen thickness
B_N	Specimen net thickness at the side groove roots
E	Elastic modulus
J	Rice J-integral
J_M	Ernst modified J-integral
J_{el}	The elastic component of J
J_{pl}	The plastic component of J
K	Stress intensity factor
K_i	Stress intensity factor at loading step i
m	Geometry factor for J_M calculation
M	Applied moment per unit thickness
P	Applied load
P_i	Applied load at loading step i
T_i	Traction on the contour Γ at point i
$\bar{u}_i$	Displacement on the contour Γ at point i

* United States Naval Academy, Annapolis, Maryland 21402, USA.
† DTRC Annapolis Laboratory, Annapolis, Maryland, 21402, USA.

W Specimen width
$\tilde{W}$ Strain energy density
ε_{ij} Strain components
δ Load point displacement
η_i Proportionality factor of J-calculation
γ_i Crack growth correction factor of J-calculation
v Poisson ratio
σ_{ij} Stress components
θ Angle of bend for a bend geometry

Introduction

The objective of this report is to present recent work which attempts to define the limits of the J-controlled crack extension in a bend type fracture mechanics test specimen. Both analytical **(1)** and computational **(2)(3)** techniques have been applied to this task in the past and have led to size criteria presently utilised in the J_{Ic} and J–R curve test standards, i.e., ASTM E813 and ASTM E1152, respectively. When applied to experimental data these limitations have not corresponded to observed experimental phenomena which could be identified as due to a loss of J-control for the particular test. This would seem to lead to the conclusion that either the J-controlled crack growth was not present before the aforementioned criteria was reached, or that it still existed after the criteria were exceeded.

Background

Observations for experiment

Experimental work was described in a previous report **(4)** in which standard unloading compliance J–R curve tests were conducted to large crack extensions. The results used the J-equations of ASTM E1152 and the J_M (J-modified) formulation of Ernst **(5)**. The observations of this previous work can be stated briefly as follows.

(1) For scaled compact specimens of materials with a range of toughnesses, the deformation J–R curve was found to be remarkably size independent to crack extensions as large as 60 percent of the initial uncracked ligament.
(2) Deformation J–R curves continued to rise even to these large crack extensions.
(3) No limit to the J-controlled crack growth was apparent for the J–R curves for any of the materials tested.
(4) The J_M–R **(4)** curves, on the other hand, demonstrated strong size dependence with small specimens developing a sigmoidal shape rising distinctly above the corresponding J_M–R curves of larger specimens. These differences amongst specimens occurred after about 30 percent of crack extension and were most distinct in the low toughness alloys.

(5) The J_M–R curves were relatively size independent only for the highest toughness alloy which exceeded all standard J-size requirements before measurable crack extension was found.

Additional experimental work performed recently has verified the above observations. A major objective of this work is to look more closely at this data set, to clarify this rather confusing situation, and where possible to generate meaningful limitations to the useful extent of the J–R curve.

Deformation J-equations

The original J-integral formulation by Rice **(6)** was that

$$J = \oint_\Gamma \left[\tilde{W}\, dy - T_i \cdot \frac{\partial \bar{u}_i}{\partial x}\, ds \right] \tag{1}$$

where

$\tilde{W} = \int \sigma_{ij}\, d\varepsilon_{ij}$ is the strain energy density
Γ = the path of the integral
ds = increment of distance along the contour Γ
$\bar{T}_i$ = tractions on the contour Γ
$\bar{u}_i$ = a displacement component in the direction of $\bar{T}_i$.

This equation is useful for analysis and for computational methods but it is not a good starting point to develop J-estimates for laboratory specimens. An equivalent form for J was presented by Rice **(7)** as

$$J = -\int_0^\delta \frac{\partial \tilde{P}}{\partial a}\, d\delta = \int_0^{\tilde{P}} \frac{\partial \delta}{\partial a}\, d\tilde{P} \tag{2}$$

where $\tilde{P}$ is the load per unit thickness applied to the specimen and δ is the resulting load point displacement.

Equation (2) was used successfully by Begley and Landes **(8)(9)** to do experimental J-integral work, but it is far from convenient. A further simplification was obtained by Rice *et al.* **(7)** who continued equation (2) with the observation that for bending geometries

$$\theta = F\left[\frac{\tilde{M}}{b^2}\right] \tag{3}$$

where b is the remaining uncracked ligament and $\tilde{M}$ is the applied moment per unit thickness, and obtained for J that

$$J = \frac{2}{b}\int_0^\theta \tilde{M} d\theta = \frac{2}{b}\int_0^\delta \tilde{P}\, d\delta \tag{4}$$

Equation (4) is only exact for the case of deeply cracked bend bars. It does relate the J-integral directly, however, to an easily measured quantity, the area under the specimen load displacement record.

For the case where crack growth was present, Ernst **(10)** developed an incremental evaluation of J which was adopted by ASTM E1152 as follows

$$J = J_{EL} + J_{PL} \tag{5}$$

$$J_{EL(i)} = \frac{(K_i)^2(1 - \nu^2)}{E} \tag{6}$$

where

$$K_i = [P_i/(BB_N W)^{1/2}] \cdot f(a_i/W) \tag{7}$$

with

$$f(a_i/W) = \frac{[(2 + a_i/W)(0.886 + 4.64a_i/W - 13.32(a_i/W)^2 + 14.72(a_i/W)^3 - 5.6(a_i/W)^4)]}{(1 - a_i/W)^{3/2}} \tag{8}$$

and

$$J_{pl(i)} = \left[J_{pl(i-1)} + \left(\frac{\eta_i}{b_i}\right)\frac{A_{pl(i)} - A_{pl(i-1)}}{B_N}\right] \cdot \left[1 - \gamma_i \frac{(a_i - a_{i-1})}{b_i}\right] \tag{9}$$

where

$$\eta_i = 2.0 + 0.522b_i/W,$$

and

$$\gamma_i = 1.0 + 0.76b_i/W. \tag{10}$$

The integration of equation (2) is obtained in equation (9) by trapezoidal approximations over which the crack length is assumed constant and small steps are required for accurate J-evaluation using this form. This becomes more crucial as the remaining ligament, b, becomes small.

Modified J-equations

More recent work by Rice *et al.* **(11)** has investigated the evaluation of J for growing cracks. Their results seem to suggest that when appreciable crack extension is present, a J-resistance curve can depend on the type and size of the specimen used for its experimental determination. Ernst **(5)** has proposed a modified J-quantity which is corrected to first order to eliminate this proposed dependence on specimen size and type. The details of this analysis are left to reference **(5)** but the resulting equation is

$$J_M = J - \int_{a_0}^{a} \left(\frac{\partial J_{pl}}{\partial a}\right)_{\delta_{pl}} da \tag{11}$$

where δ_{pl} is the plastic component of the applied load line displacement. Ernst simplifies this for experimental geometries by substituting the approximate

relationship that

$$\left(\frac{\partial J_{pl}}{\partial a}\right)_{\delta_{pl}} = -m\frac{J_{pl}}{b} \tag{12}$$

where m is a function of crack length and specimen geometry to give

$$J_M = J + \int_{a_0}^{a} \frac{m}{b} J_{pl}\, da \tag{13}$$

In the sections that follow, both J and J_M-resistance curves are evaluated for large crack extensions for compact specimens of a range of sizes and toughnesses. These evaluations are carried out well beyond accepted J and crack extension limits and the results need careful critical appraisal.

Experimental procedure

On the presence of a singularity

The presence of a singularity in an elastic–plastic fracture toughness specimen is difficult to experimentally verify. Computational techniques **(12)** do verify the path independence of J and the equivalence of the various equations for its evaluation. The analysis of Paris and Hutchinson **(13)** argues that if strain components remain proportional, the J-controlled crack growth can, in fact, exist, but does not identify to what extent growth consistent with a J-control might exist for a given specimen configuration.

Since the non-linear elastic J-integral singularity reduces to the elastic stress intensity factor for cases of fully elastic material behaviour, and the singularity has been well verified, it certainly seems likely that a J-singularity might exist for low toughness materials, for limited amounts of crack growth. Such a singularity should act to produce the most intense conditions for crack growth, and as the singularity weakens, the amount of crack growth per increment of specimen deformation should be reduced as well.

Material and specimen characterisation

The three materials analysed in this report are a 3 percent Nickel alloy steel, an A710 high strength low alloy steel, and an A533B pressure vessel steel. The tensile mechanical properties of these steels are shown in Table 1 and the chemistries are shown in Table 2. All specimens were 1/2T, 1T, or 2T compact specimens. All specimens included in this study had thickness dimensions of

Table 1 Tensile properties for alloy steels 70°F

	Code	*0.2% Yield strength MPa*	*Tensile strength MPa*	*% Elongation (50 mm)*	*% R.A. (12.5 mm)*
3% nickel	FYB	614	732	32	80
A710	GFF	511	601	23	63
A533B	H13	443	622	26	60

Table 2 Chemical composition of alloys (Wt percent)

	C	*Mn*	*P*	*S*	*Cu*	*Si*	*Ni*	*Cr*	*Mo*	*V*	*Ti*	*Cb*
3% nickel	0.153	0.33	0.012	0.012	0.033	0.18	2.55	1.66	0.37	0.003	<0.001	—
A710	0.04	0.59	0.005	0.004	1.17	0.25	0.90	0.70	0.19	0.003	0.06	0.03
A533B-H13	0.19	1.28	0.012	0.013	—	0.21	0.64	—	0.55	—	—	—

0.5W and all were side grooved with a 45 degrees included angle Charpy notch with a 0.25 mm radius to a total reduction of 20 percent. The A710 and 3 percent Nickel alloys were tested in the T–L orientation while the A533B steel was tested in the L–T orientation. All tests were performed using an unloading compliance technique according to ASTM E1152 except that the loading was continued until large crack extensions were present.

Normalised load displacement records

Data plots which have been looked at to try to gain insight into the existence of a singularity using the data of reference **(4)** are shown in Figs 1–2. On these figures a normalised load, PW/Bb^2, is plotted versus δ_{pl}/W and it can be seen that this format causes the load displacement relationships of various sizes of specimens to plot on a single curve. The three curves in each case demonstrate that this result is insensitive to the material toughness and yield strength, specimen size, and crack length. This formulation is a useful observation and

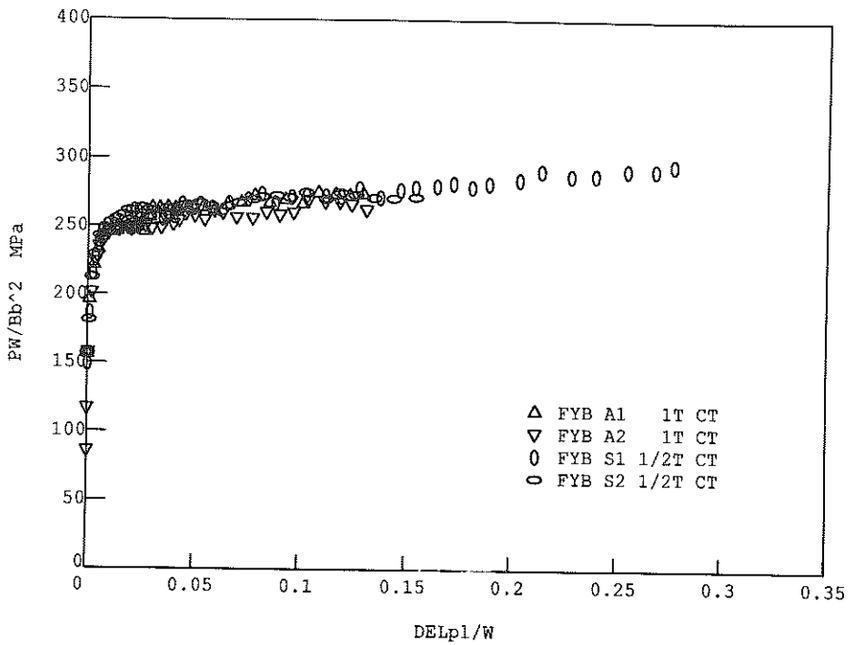

Fig 1 Key curve normalised plot for the 3 percent nickel alloy (FYB)

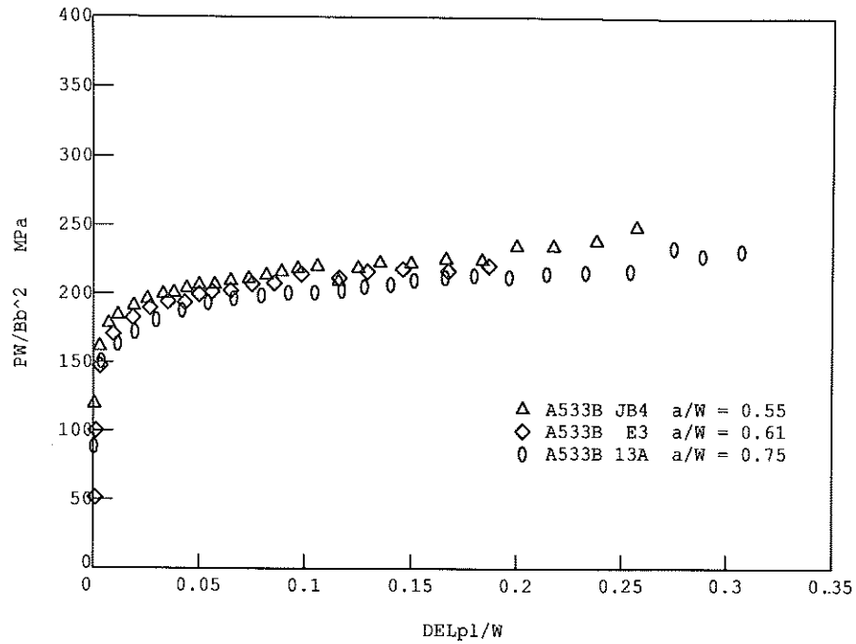

Fig 2 Key curve normalised plot for the A533B-H13 alloy

will be utilised further below, but it does not yield directly any insight into the presence or absence of a singularity for these materials.

The singularity expected near an elastic–plastic notch or crack tip would be predominantly a strain singularity. The experimentally measured load is thus likely to be very weakly dependent on whether or not a singularity is present at a crack tip in a standard test geometry. On the other hand, if the specimen is at its limit load, this is no guarantee that a strain singularity is not still present and controlling the local conditions for crack growth.

J-resistance curves

Figures 3–8 show typical deformation *J*- and modified *J*-resistance curves presented previously **(4)**. Here the deformation *J*–*R* curves seem to maintain the desired uniformly rising shape and are consistent for various specimen sizes. The modified *J*-resistance curves, on the other hand, show a tendency to rise after approximately 30 percent growth of the crack has occurred, and the resulting resistance curves are then strongly size dependent. Careful crack length measurements, and blunt notch specimen tests, were done as part of the work in reference **(4)** to verify the accuracy of the *J*-resistance curves developed, and this work has shown that accuracies of both *J* and Δa should be within 10 percent even after the large crack extensions had occurred.

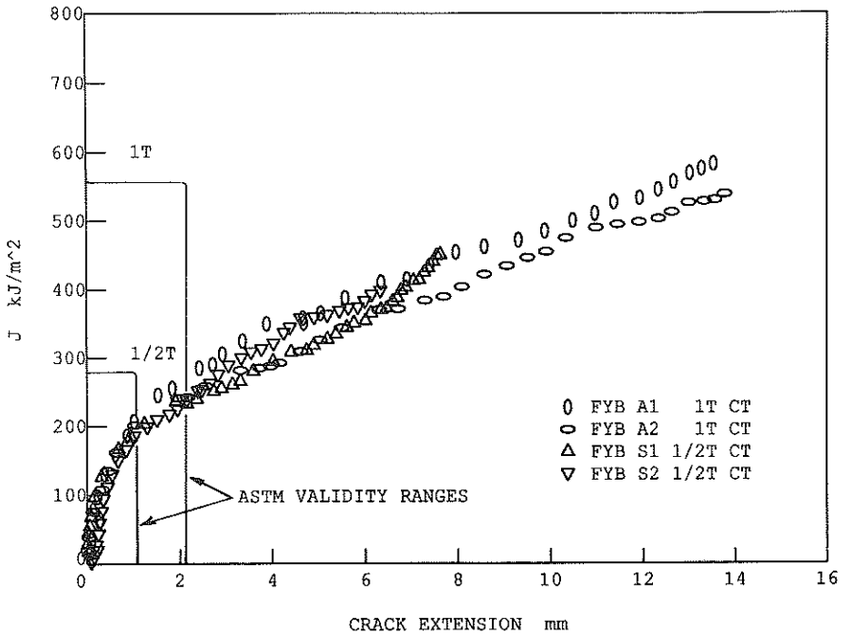

Fig 3 Deformation *J*-resistance curves to large crack extensions for the 3 percent nickel alloy

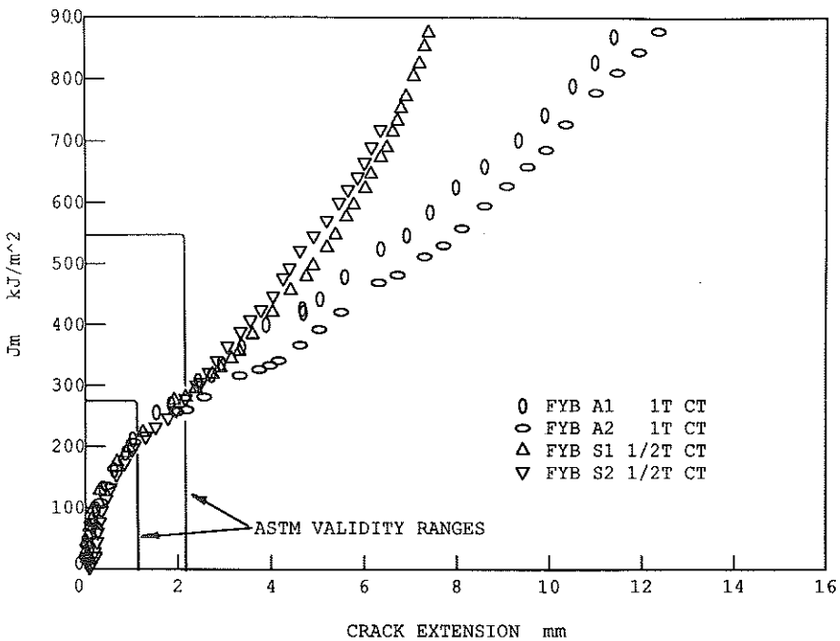

Fig 4 Modified *J*-resistance curves to large crack extensions for the 3 percent nickel alloy

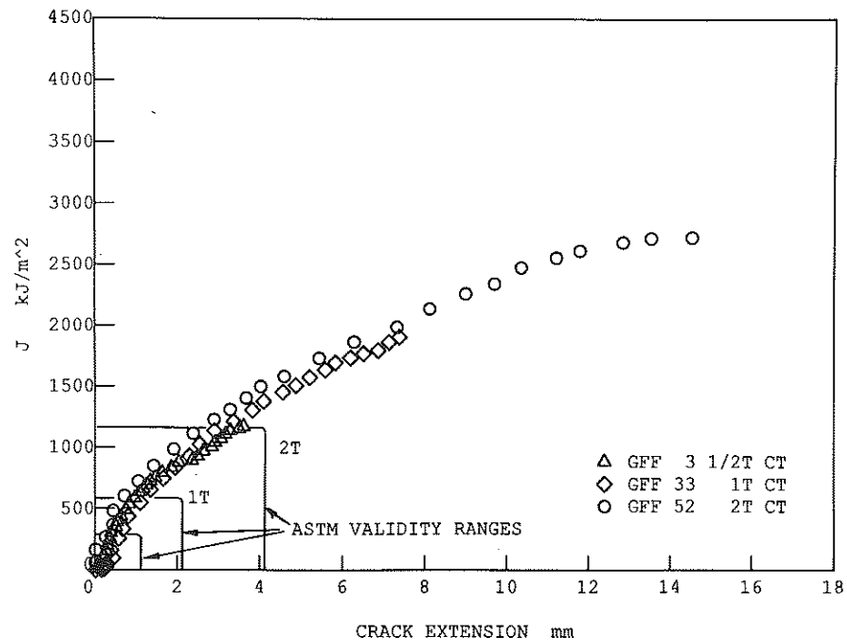

Fig 5 Deformation *J*-resistance curves to large crack extensions for the A710 alloy

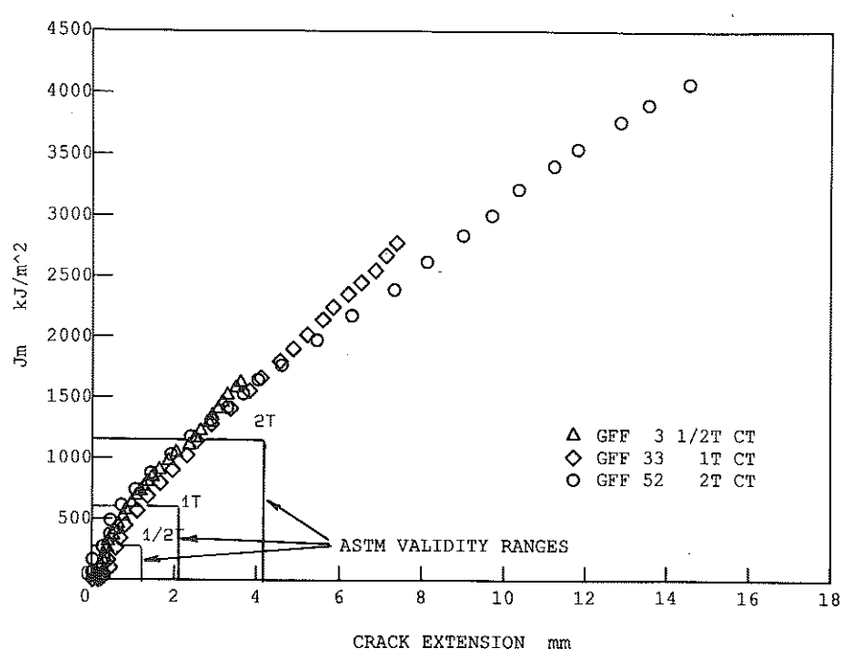

Fig 6 Modified *J*-resistance curves to large crack extensions for the A710 alloy

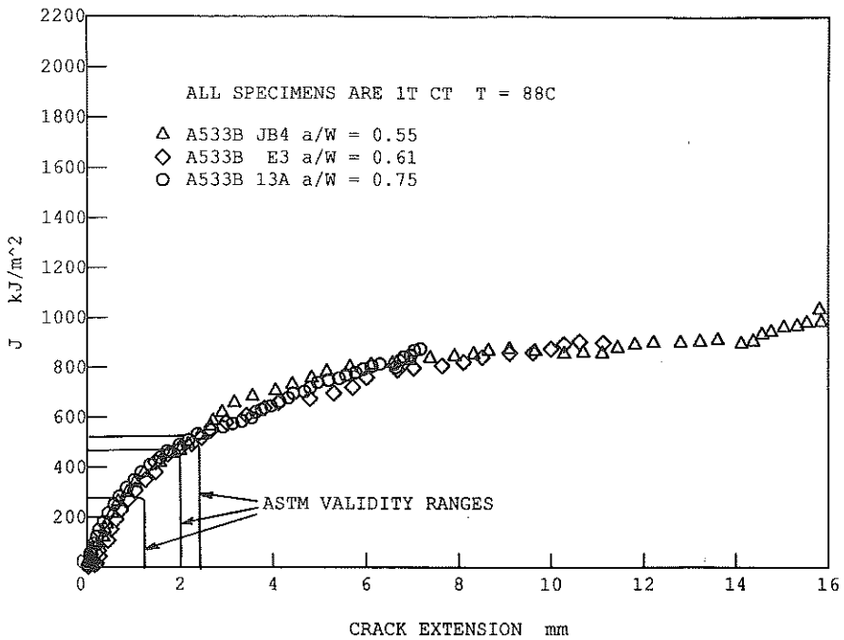

Fig 7 Deformation *J*-resistance curves to large crack extensions for the A533B-H13 alloy

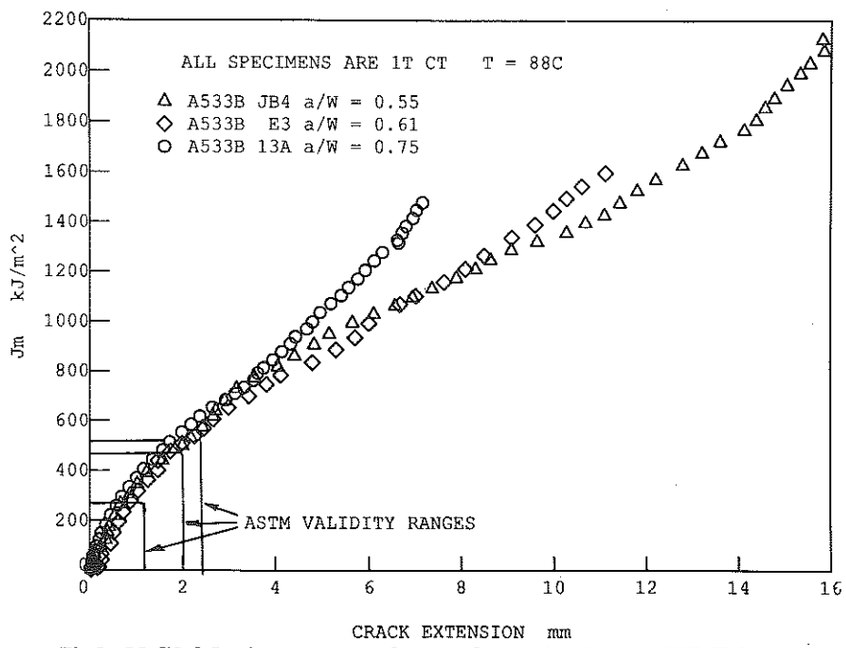

Fig 8 Modified *J*-resistance curves to large crack extensions for the A533B-H13 alloy

For the lower toughness materials, like the 3 percent Nickel steel of Fig. 3, a *J*-singularity is expected for the initial region of crack growth, but as shown, the *J*–*R* curve continues to consistently rise to large *J*-values and large amounts of crack extension. The labelled boxes on the figures show the valid ASTM E1152 regions presently thought to define bounds to the region of *J*-controlled growth. Nothing seems to occur on the *J*-deformation resistance curve which could be taken to imply a loss of *J*-control even well beyond this 'valid' box. Does the *J*-control not exist inside the box? Does the *J*-control continue to exist outside the box? How can one define meaningful engineering limits to the region of *J*? These questions need a more complete answer before *J* is used in critical fracture analyses, and a partial answer now seems to be forming – as shown in the next section.

Definition of a region of J*-control*

Figure 9 shows a typical plot of the normalised crack opening displacement versus normalised crack extension for various size specimens of the 3 percent Ni material.

Figure 9 shows a region of initial crack blunting, followed by a region of intense crack growth, which is then followed by a third region of ever slower crack extension. This type of plot is referred to below as a 'crack growth

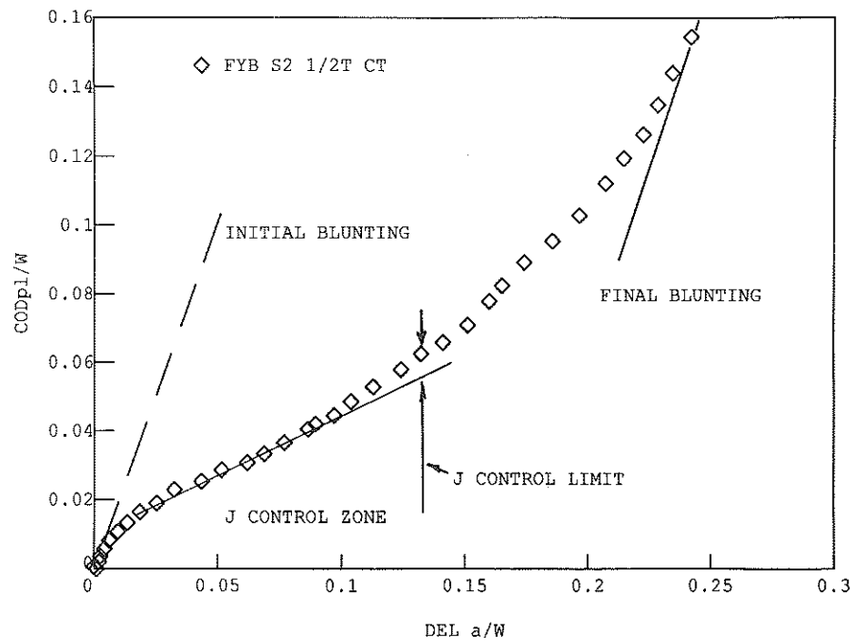

Fig 9 Definition of an engineering *J*-control limit in terms of the loss of intense crack growth

intensity plot' because it defines the regions of crack growth by blunting and of J-controlled (i.e., intense) crack growth. It is not possible at this stage to formulate a clear distinction between crack blunting and crack extension. Generally crack blunting in this work corresponds to crack growth in which the crack tip opening is approximately equal to, or greater than, the crack extension directly ahead of the original crack tip. This case then corresponds to a crack developing into a blunted notch geometry and 'growing' by a gross necking of the specimen remaining ligament.

Crack extension is the alternative where the crack tip opening displacement is less than the crack extension, a phenomenon which would seem to relate to an intense stress on strain field at the crack tip.

After the initial period of crack blunting, a transition occurs as shown in Fig. 9. This transition includes the start of J-controlled crack growth, and beyond this point there is at least a region of crack growth during which blunting is negligible and somewhat uniform crack growth conditions prevail. This is the region of intense crack growth for this specimen, and the constant slope in this region corresponds to nearly constant crack increments per step of specimen plastic deflection. At some point, labelled the 'J-control limit' in Fig. 9, the data starts to become elevated as the specimen returns to a blunting behaviour labelled 'final blunting' in Fig. 9. This transition back to predominantly blunting crack extension is gradual and defining a limit to J-control is somewhat arbitrary, but nonetheless necessary. Plots of this form have been

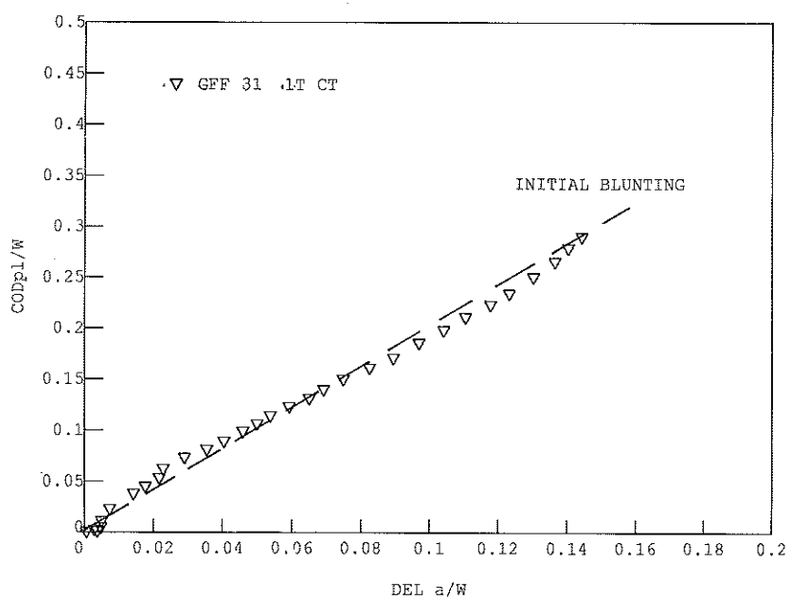

Fig 10 Blunting only behaviour as demonstrated by the high toughness A710 alloy

obtained on a large number of specimens of different materials, geometries, and configurations and results consistent with the above pattern have been found in all cases.

For high toughness alloys, or for very small specimens, the J-controlled crack growth region never forms, as shown in Fig. 10 for the A710 alloy. It appears that for this high toughness material, a region of J-controlled crack extension never forms, and the crack grows only by crack blunting. Nonetheless a major change in crack length takes place, but always with the crack tip forward progress staying on the order of the CTOD, so that the crack moves forward only as a blunted notch. If specimens of various scales are plotted for the A710 alloy, all sizes produce similar results as shown in Fig. 11. The initial blunting line plotted in Figs 9–11 is taken to have the functional form.

$$\frac{\delta_{pl}}{W} = 2\,\frac{\Delta a}{W} \tag{14}$$

The slope of 2 was chosen to correspond to the data of the high toughness A710 alloy and is used for comparison on subsequent plots.

The fact that the results in Fig. 11 scale with specimen dimension W demonstrates that this material, in these specimen sizes, never achieves intense, J-controlled, crack extension conditions, i.e., blunting or ligament necking is the only crack growth mechanisms that occurs in this case.

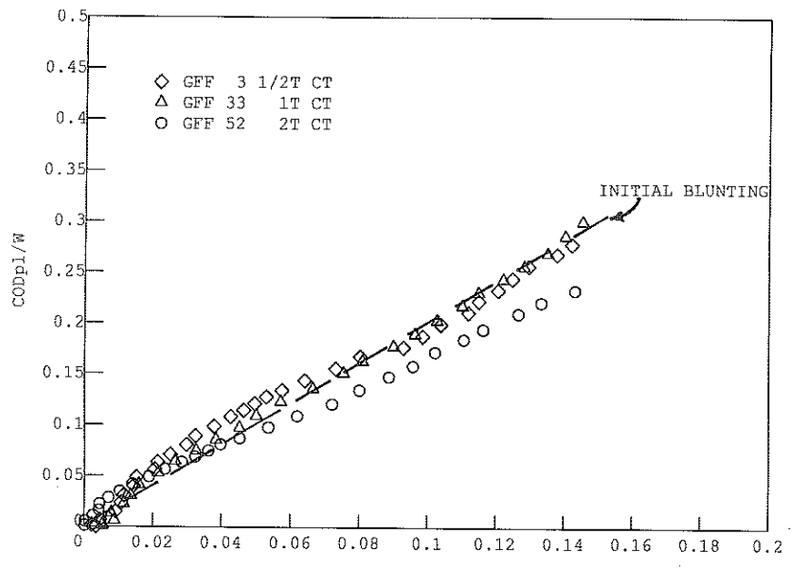

Fig 11 The effect of specimen size on the plot of δ_{pl}/W versus crack extension for the high toughness alloy

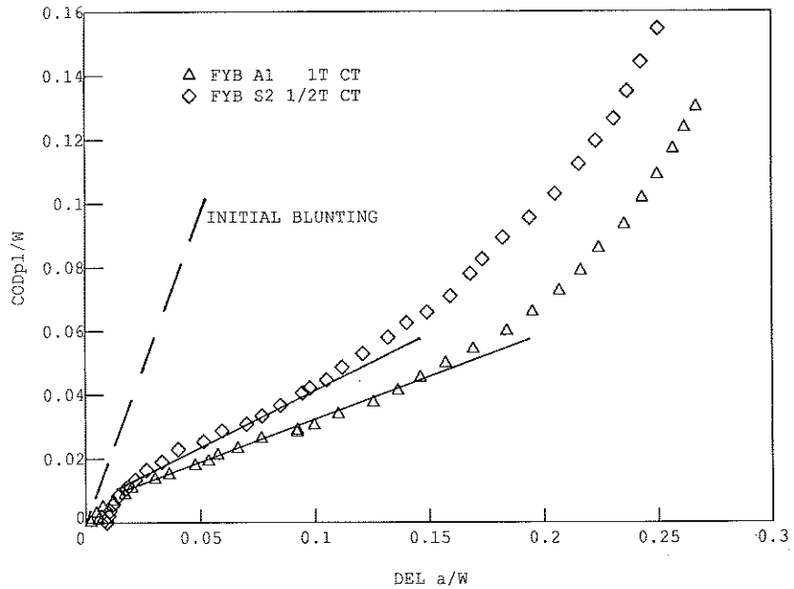

Fig 12 The effect of specimen size on the plot of δ_{pl}/W versus crack extension for the low toughness alloy

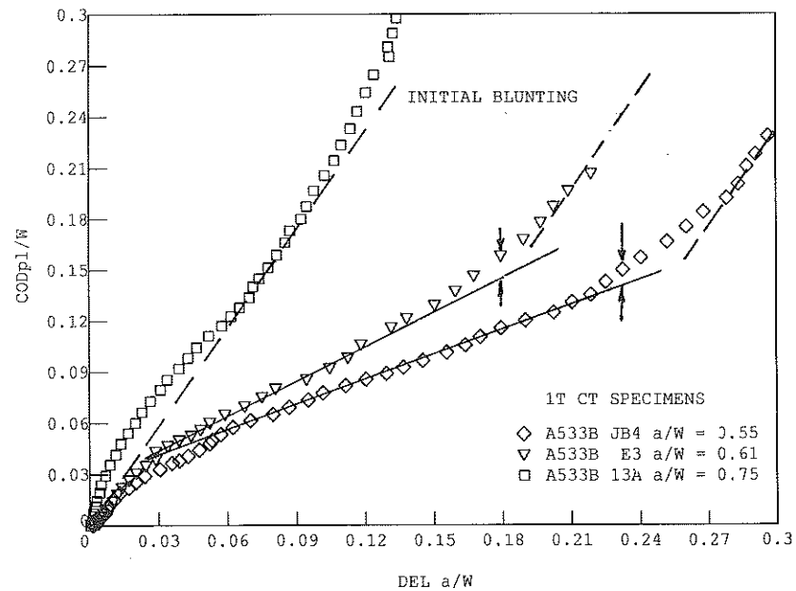

Fig 13 The specimen crack length is shown to have a strong effect on the *J*-controlled crack growth limit

When a region of *J*-controlled crack growth exists, as is the case for the FYB alloy, different size specimens give different crack growth intensity curves as shown in Fig. 12. Generally larger specimens have *J*-control regions with flatter slopes and the *J*-control regions extend to larger $\Delta a/W$ values. Similarly when different a/W ratios are present, different crack growth intensity curves result as shown for the A533B alloy in Fig. 13. Here shorter crack lengths give more intense *J*-control regions (lower slopes) than larger crack lengths. In both of these cases consistent *J*–*R* curves were evaluated for the various specimen sizes and crack lengths.

For the data sets of Figs 3 and 7, consistent deformation *J*-resistance curves are found even when data beyond the *J*-control limit of Fig. 9 is included. This result appears to be fortuitous for these cases and certainly is not always the case. This is shown dramatically in Figs 14 and 15 where data from FYB 1T CT specimens are plotted, first as deformation *J*-resistance curves and then as crack growth intensity curves. The *J*–*R* curves appear to be very geometry dependent in Fig. 14, but if data beyond the *J*-control limit, obtained from Fig. 15 and shown by solid points, are eliminated, a very consistent family of *J*–*R* curves results.

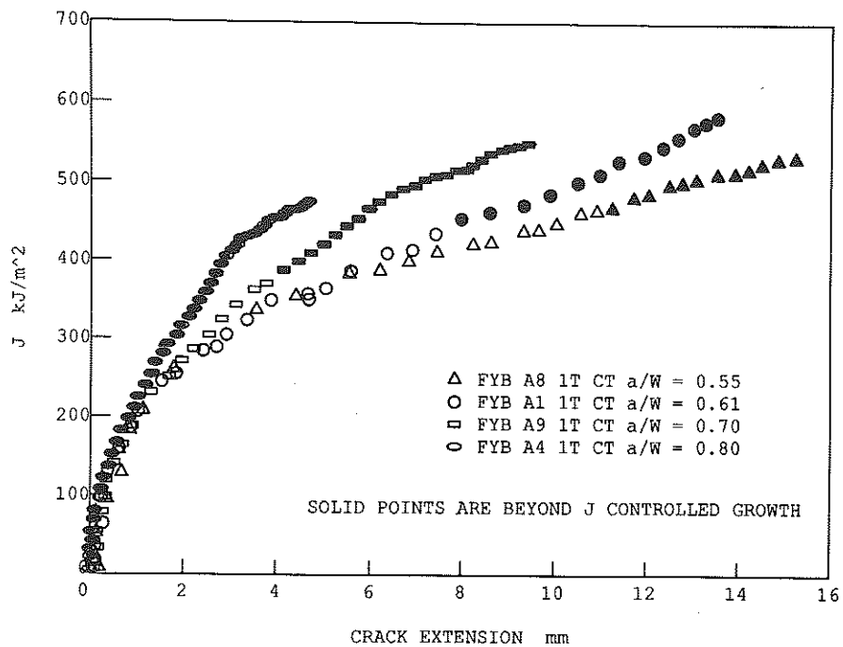

Fig 14 *J*-deformation *J*–*R* curves to large crack extensions showing the deviations present beyond *J*-control

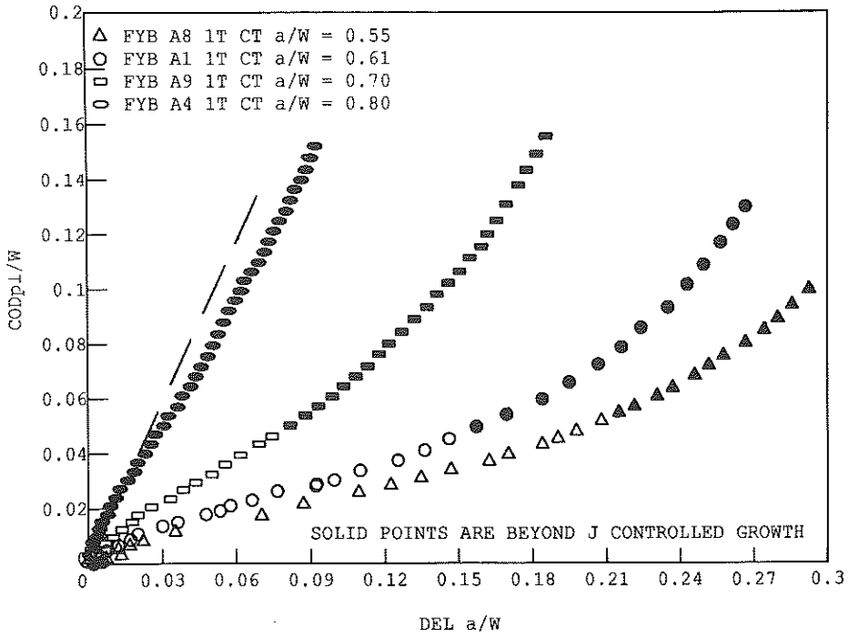

Fig 15 Definitions of *J*-control for the samples with varied *a/W* ratios

Conclusions

Limits to the engineering applicability of *J*-resistance curves are not experimentally determinable in terms of load dominated quantities like key curve plots or *J*-resistance curves. This apparently is so because laboratory specimens generally attain limit load whether *J*-controlled crack growth conditions are present or not.

Limits to the applicability of the *J*-integral are much more apparent in a plot of the plastic component of crack mouth opening displacement or specimen bend angle versus normalised crack extension. These plots show a region of initial crack blunting, a region of *J*-controlled crack growth (when it exists) and finally a gradual return to crack blunting. Limits to the extent of 'engineering' *J*-control can be established in terms of these data. In this work a straight line is made to fit the data in the '*J*-controlled' zone and a deviation of data from this line is taken to mark the limit of *J*-control for an individual specimen.

The specimen size dependence demonstrated by the modified *J* of Ernst appears to correspond to a loss of *J*-control in these specimens and hence acts as another method to define the engineering limit to *J*-controlled crack growth. This observation means that both deformation *J* and modified *J* are specimen size and geometry independent when engineering *J*-control conditions are present as defined by the above criteria.

When data are beyond the *J*-controlled region deformation *J*-resistance curves can curve up, curve down, or stay consistent with *J*-controlled data. Elimination of data beyond *J*-control growth is recommended to obtain consistent and meaningful results.

These results, then, do not show a preference for deformation *J* or *J*-modified. They show that the range of *J*-control, expressed in terms of either of these parameters is similar, i.e., use of *J*-modified does not extend the useful range of experimental *J*-resistance curves. The upward deviation of J_m-resistance curves of small specimens, in comparison with large specimens is not, then, a true size dependence but only a measure of the limit of applicability for the small specimen J_m–R curve.

The choice between deformation *J*-resistance curves and *J*-modified resistance curves will depend on the results of large-scale tearing instability tests which hopefully will demonstrate which resistance curve formulation properly predicts the onset of tearing instability.

References

(1) PARIS, P. C. (1972) Discussion to J. A. Begley and J. D. Landes, *Fracture Mechanics*, ASTM STP *514*, pp. 21–22, ASTM, Philadelphia.
(2) SHIH, C. F., deLORENZI, H. G., and ANDREWS, W. R. (1979) Studies on crack initiation and stable crack growth, *Elastic–Plastic Fracture*, ASTM STP *668*, (Edited by J. D. Landes, J. A. Begley, and G. A. Clarke), pp. 65–120, ASTM, Philadelphia.
(3) BOOTH, B. C., NEWMAN, J. C., JR., and SHIVAKURMAN, K. N. (1985) An elastic–plastic finite-element analysis of the *J*-resistance curve using a CTOD criterion, *ASTM 18th Nat. Symposium on Fracture Mechanics*, Boulder, CO.
(4) JOYCE, J. A., DAVIS, D. A., HACKETT, E. M., and HAYS, R. A. (1988) Application of the *J*-integral and modified *J*-integral to cases of large crack extension, *NUREG/CR5143*, USNRC, Washington, D.C., 20555.
(5) ERNST, H. A. (1983) Material resistance and instability beyond *J*-controlled crack growth, *Elastic–Plastic Fracture: Second Symposium, I – Inelastic Crack Analysis*, ASTM STP *803*, (Edited by C. F. Shih, and J. P. Gudas), I-191–I-213, ASTM, Philadelphia.
(6) RICE, J. R. (1968) A path independent integral and the approximate analysis of strain concentration by cracks and notches, *J. App. Mech.*, **35**, 379–386.
(7) RICE, J. R., PARIS, P. C., and MERKLE, J. G. (1973) Some further results of *J*-integral analysis and estimates, *Progress in Flaw Growth and Fracture Toughness Testing*, ASTM STP *536*, pp. 231–245, ASTM, Philadelphia.
(8) BEGLEY, J. A. and LANDES, J. D. (1972) The *J*-integral as a fracture criterion, *ASTM STP 514*, pp. 1–20, ASTM, Philadelphia.
(9) LANDES, J. D. and BEGLEY, J. A. (1973) Test results from *J*-integral studies: an attempt to establish a J_{Ic} testing procedure, *ASTM STP 560*, pp. 170–186, ASTM, Philadelphia.
(10) ERNST, H. A., PARIS, P. C., and LANDES, J. D. (1981) Estimations on *J*-integral and tearing modulus T from a single specimen test record, *Fracture Mechanics: Thirteenth Conference, ASTM STP 743*, Roberts, R. Ed., pp. 476–502, ASTM, Philadelphia.
(11) RICE, J. R. and SORENSEN, E. P. (1978) *J. Mech. Phys. Solids*, **26**, 163–816.
(12) BAKKER, A. (1984) The three-dimensional *J*-integral, *WTHD* **167**, Depart. of Mechanical Engineering, Delft University of Technology, Delft, Netherlands.
(13) HUTCHINSON, J. W. and PARIS, P. C. (1979) Stability analysis of *J*-controlled growth, *ASTM STP 668*, pp. 37–64, ASTM, Philadelphia.